THE ASTROPHYSICAL JOURNAL, 287:761–768, 1984 December 15

THE EVOLUTION OF THE INNER REGIONS OF VISCOUS ACCRETION DISKS SURROUNDING NEUTRON STARS[1]

RONALD E. TAAM
Northwestern University

AND

D. N. C. LIN
Lick Observatory

Received 1984 April 23; accepted 1984 June 25

ABSTRACT

The structure and evolution of the inner regions of an accretion disk surrounding a neutron star has been investigated subject to variations in the mass flow rate. In order to examine the sensitivity of the global response of the disk to the form of the viscous dissipation several prescriptions based upon the α model have been adopted. We show that under certain circumstances the role of nonlocal energy transfer in the radial direction can be important in stabilizing regions of the disk which are predicted to be unstable by a local analysis. Thus a global analysis does not necessarily confirm expectations based upon a local analysis. However, in the case where the viscous stress scales with the total pressure, the global analysis confirms the results inferred from the local analysis, and the instability manifests itself in terms of short time scale (<10 s) luminosity fluctuations or bursts. A detailed study of the burst in its limit cycle reveals that the disk remains optically thick and geometrically thin throughout the evolution. Our theoretical results bear suggestive resemblance to the general observational characteristics of the rapid X-ray burster.

Subject headings: stars: accretion — stars: neutron — X-rays: bursts

I. INTRODUCTION

The structure and evolution of accretion disks is central to our understanding of diverse astronomical phenomena. Among the many examples that may be cited for supporting this statement are the accretion disks in interacting binary systems. Ever since the early work of Prendergast and Burbidge (1968), theories for accretion disks have been advanced to explain the nature of stellar X-ray sources. The generally accepted model for the binary X-ray sources consists of a close binary system in which mass is transferred from a normal, nondegenerate star toward a compact companion (neutron star or black hole). As the matter falls onto the compact component, its kinetic energy is converted into thermal energy, and X-rays are emitted. If this matter has a high specific angular momentum with respect to the compact object, a thin orbiting ring of gas will form. Internal torques resulting from viscous stresses in the ring redistribute the angular momentum and broaden the ring. Since the gas cools efficiently the ring evolves into a geometrically thin disk. A small fraction of the gas moves outward to carry the angular momentum given up by the gas which has moved inward. Hence, due to the action of viscosity, matter slowly spirals toward the stellar surface of the compact object with the loss in its binding energy efficiently converted into X-ray radiation.

From this discussion it is clear that the structure and time scale of evolution of the accretion disk is determined by the magnitude and functional form of the viscosity. Since ordinary molecular or ion viscosity cannot provide mass transport at the rate inferred for the binary X-ray sources, many investigators (Prendergast and Burbidge 1968; Shakura and Sunyaev 1973; Lynden-Bell and Pringle 1974) have assumed that the disk is turbulent and have modeled the viscosity in terms of a mixing length theory. This has become the standard (or α) disk model. For a recent review of accretion disk theory, see the paper by Pringle (1981). Early in the last decade Pringle and Rees (1972), Shakura and Sunyaev (1973), and Novikov and Thorne (1973) constructed α disk models and showed that X-ray radiation is naturally produced in the accretion disk surrounding a black hole. In these simplified steady state models, the mass flow rate was assumed to be independent of time and of distance from the central object. Subsequently, it was shown, within the context of accretion disks surrounding a collapsed object, that the inner region of the α disk is unstable to thermal and surface density perturbations (Pringle, Rees, and Pacholczyk 1973; Lightman and Eardley 1974). Both types of instability can arise when radiation provides the major contribution to the total pressure (Shakura and Sunyaev 1976). The thermal instability results from the inability of the local heating and cooling mechanisms to efficiently maintain a thermal balance, while the viscous instability results from a "negative" diffusion coefficient which amplifies density contrasts. In the former case the inner region of the disk heats up and may become geometrically thick, whereas in the latter case the disk tends to break up into concentric rings. In circumstances where the disk is unstable to both thermal and surface density perturbations, thermal instability determines the evolution of the disk since its corresponding growth time is shorter.

It is quite possible that these types of instabilities may be responsible for the short time scale variability seen from objects such as Cyg X-1 and the rapid burster MXB 1730−335. In the case for Cyg X-1, such instabilities are prime candidates for the millisecond-to-second X-ray fluctuations (Shakura and Sunyaev 1976). In the case of the rapid burster the persistent emission is not steady, and it is thought that the modulations in the accretion flow due to a magnetic gate mechanism (Lamb *et al.* 1977) or instabilities in the disk (Liang

[1] *Lick Observatory Bulletin*, No. 998.

1977) may be the primary cause. The duration of the bursts from the rapid burster are variable ranging from seconds to minutes (Lewin *et al.* 1976; Oda 1982) which may either reflect the development of the instability over regions of the disk which are different in radial extent or indicate that the magnetic gate can be kept open for a range of time scales. These bursts, which are known as type II bursts, are not thermonuclear in origin since there is insufficient time between successive bursts to accumulate matter to reinitiate the next burst. For a review of the properties of the rapid burster see the review by Lewin and Joss (1981). Thus, there is some observational motivation for studying these instabilities; however, as has been stressed in the literature such instabilities may not be real, but rather they may reflect inconsistencies in the steady state disk structure. Modifications in the prescription for the viscosity law can render the disk stable to both thermal and viscous processes (Piran 1978). For example, the disk can be stabilized with respect to surface density perturbations if the viscous stress is scaled to the gas pressure instead of the total pressure (Lightman and Eardley 1974).

A major shortcoming of the stability analyses is that they are local in nature and, therefore, do not take account of the global response of the disk. In addition, the analyses are linear. Nonlinear effects must eventually limit the growth of the unstable modes. To determine whether the disk is unstable or evolves to another state requires an examination of the time dependence in the problem (Lightman 1974). Recent work by Papaloizou, Faulkner, and Lin (1983) along these lines, in the context of dwarf novae, has demonstrated that thermal instabilities, associated with the strong temperature dependence of the H^- opacity, can propagate through part of and in some cases throughout the entire disk. It is the purpose of this paper to report on an analogous investigation of the time dependent evolution of an accretion disk in cases where local analysis predicts instability in the inner region of the disk near the surface of a neutron star to determine whether such disks evolve to a steady state or to a limiting cyclic state. We shall examine viscosity prescriptions in which the viscous stress scales with the total pressure (standard model), with the gas pressure, and with some combination of the two. In the next section the basic time dependent differential equations and constitutive relations are presented. The approximate steady state solutions for the inner region of the disk are reviewed and summarized in § III. The results of our numerical calculations are presented and compared with the steady state solutions in § IV. Finally we discuss the implications of the results and make some concluding remarks in § V.

II. FORMULATION OF THE PROBLEM

We assume that the only source of gravity is that due to the compact object. The gravitational effect of the companion star and the self gravity of the disk are small in comparison and are neglected. Considerations based upon conservation of mass and angular momentum yield the standard time-dependent mass diffusion equation (Lynden-Bell and Pringle 1974):

$$\frac{\partial \Sigma}{\partial t} = \frac{3}{r}\frac{\partial}{\partial r}\left[r^{1/2}\frac{\partial}{\partial r}\left(\nu \Sigma r^{1/2}\right)\right], \tag{1}$$

where $\Sigma(r)$ and ν are the surface density of the disk at a given cylindrical radial coordinate and the effective kinematic viscosity, respectively. In equation (1), it is implicitly assumed that the gas orbits a central point mass, M, in Keplerian motion. The effective kinematic viscosity is parameterized in terms of α ($\lesssim 1$) and, based upon dimensional arguments, is of the form

$$\nu = \tfrac{2}{3}\alpha C_s H , \tag{2}$$

where C_s is the local speed of sound and H is the local vertical pressure scale height in the disk. If we make the assumption that the disk is in vertical hydrostatic equilibrium and is geometrically thin (so that the gravitational potential may be approximated by a quadratic function of height above and below the midplane) we can rewrite equation (2) as

$$\nu = \frac{2}{3}\frac{\alpha C_s^{\,2}}{\Omega} , \tag{3}$$

where Ω is the Keplerian angular velocity at a given radius equal to $(GM/r^3)^{1/2}$.

Time dependence must also be included in the energy transport equation. Following Faulkner, Lin, and Papaloizou (1983), conservation of energy yields

$$C_v\rho\left[\frac{\partial T}{\partial t} + v\frac{\partial T}{\partial r} - (\Gamma_3 - 1)\frac{T}{\rho}\left(\frac{\partial \rho}{\partial t} + v\frac{\partial \rho}{\partial r}\right)\right] = D - \frac{1}{r}\frac{\partial r F_r}{\partial r} - \frac{\partial F_z}{\partial z} , \tag{4}$$

where C_v, ρ, T, Γ_3, v, D, and F are the specific heat at constant volume, the gas density, temperature, adiabatic exponent, radial velocity, energy generation rate per unit volume, and radiative flux, respectively. In equation (4) the advection of energy by mass motion in the radial direction as well as radiative diffusion in the vertical and radial directions are explicitly included. The energy generated per unit volume per unit time by viscous dissipation is given from fluid dynamics as

$$D = \tfrac{9}{4}\rho\nu\Omega^2 . \tag{5}$$

To simplify the (inherently) two-dimensional problem, we average equation (4) over the vertical direction. The energy balance equation can now be written as

$$C_v\left[\frac{\partial T_c}{\partial t} + v\frac{\partial T_c}{\partial r} - (\Gamma_3 - 1)\frac{T_c}{\Sigma}\left(\frac{\partial \Sigma}{\partial t} + v\frac{\partial \Sigma}{\partial r}\right)\right] = \frac{9}{4}\nu\Omega^2 - \frac{2H}{\Sigma r}\frac{\partial r F_r}{\partial r} - \frac{2F_z}{\Sigma} , \tag{6}$$

where we have replaced the temperature by its midplane value and have used $\Sigma = 2\rho H$. Since the disk is geometrically thin, the energy generated by viscous dissipation is primarily transported vertically outward by radiative processes. If the root mean optical depth, $\tau_{\rm eff}$, is much greater than unity, the radiation intensities approach the Planck function. Here, $\tau_{\rm eff}$ is given as

$$\tau_{\rm eff} = (\kappa_e \kappa_{\rm ff})^{1/2}\frac{\Sigma}{2} , \tag{7}$$

where the opacity due to free-free absorption and electron scattering are

$$\kappa_{\rm ff} = 6.13 \times 10^{22}\rho T^{-7/2} \tag{8}$$

and

$$\kappa_e = 0.34 . \tag{9}$$

In equations (8) and (9) Population I abundances ($X = 0.7$, $Y = 0.28$, $Z = 0.02$) have been adopted. Contributions to the opacity due to bound-free processes have been neglected since we are primarily interested in the cases where the disk is fully ionized. The flux, F, emitted from one surface of the disk is, then, in the diffusion approximation given as

$$F_z = \frac{2acT_c^4}{3(\kappa_{\rm ff} + \kappa_e)\Sigma} . \tag{10}$$

If the effective optical depth is less than unity, the radiation is no longer in local thermal equilibrium and the gas does not radiate as a blackbody (i.e., the disk becomes locally optically thin). The energy will be emitted as bremmstrahlung radiation unless electron scattering is important. For most cases, however, the electron scattering optical depth is much greater than unity and the radiative flux may be Compton enhanced. The expression for the radiative flux in the optically thin limit is taken from Illarionov and Sunyaev (1974) and is

$$F_z = \epsilon_{\rm ff} AH , \tag{11}$$

where A is the Compton enhancement factor, and $\epsilon_{\rm ff}$ is the bremmstrahlung energy loss rate. The loss rate, $\epsilon_{\rm ff}$, is adopted from Tucker (1975) and is

$$\epsilon_{\rm ff} = 6.22 \times 10^{20}\rho^2 T^{1/2} . \tag{12}$$

The degree of Compton enhancement depends upon the Compton y parameter, where y is defined as

$$y = \frac{\tau_e^2 kT}{m_e c^2} . \tag{13}$$

For $y > 1$, A is given as

$$A = \tfrac{3}{4} \ln^2 (2.35/\zeta_e) , \tag{14}$$

where

$$\zeta_e \equiv \frac{hv_e}{kT} = 3.8 \times 10^{17}\rho^{1/2}T^{-9/4}$$

is the frequency for which inverse Compton effects can be important. If $y < 1$, we adopt the expression for A as given by Meier (1982) with

$$A = \tfrac{3}{4} y \ln^2 (2.35/\zeta_*) , \tag{15}$$

where

$$\zeta_* = 1.9 \times 10^{12}\rho^{3/2}T^{-7/4}H$$

is the frequency for which the medium becomes effectively optically thin. If the enhancement factor in equation (14) or (15) becomes less than unity, we set $A = 1$. Whenever $A\tau_{\rm eff}^2 > 1$, we use the diffusion approximation for the radiative flux and an interpolation between the Compton-enhanced flux and the diffusion approximation for $A\tau_{\rm eff}^2 < 1$. For the radiative flux in the radial direction we adopt

$$F_r = \frac{-4acT^3}{3\kappa\rho}\frac{\partial T}{\partial r} \tag{16}$$

In the optically thick regions. For optically thin regions, the radiative flux in the radial direction is set to zero.

In optically thick circumstances, the equation of state includes contributions from a fully ionized gas and radiation. When the effective optical depth is less than unity, the contribution of radiation to the pressure is negligible, since there is little energy density in the radiation field.

The outer boundary is treated as in Papaloizou, Faulkner, and Lin (1983). In particular we adopt the condition that the mass flow rate is independent of radial coordinate for the three outermost zones. Mass is then introduced at the outer boundary of the calculated disk at a constant rate independent of time. The inner boundary is formulated so that the matter at the inner disk radius is accreted by the star at a rate given by the surface density and temperature at the innermost zone. In particular, we assume that the column density vanishes at 2.67×10^6 cm (which is interior to our inner boundary). Finally, the temperature at the inner boundary is assumed to be given by local energy balance with the viscosity determined by the gas pressure alone.

III. STEADY STATE SOLUTIONS FOR THE INNER REGION

In order to relate the results of the numerical simulations to the steady state solutions, we list the latter for various regimes (see, for example, Shakura and Sunyaev 1973). In the following, we express the mass of the neutron star, M, in units of a solar mass, the mass accretion rate, $\dot{M}$, in units of 10^{16} g s^{-1}, and the radius, r, in units of 10^6 cm. The radius of the neutron star is taken to be equal to 1 in dimensionless units. Since we are primarily interested in the inner regions of the α disk, we do not list all possible solutions.

For optically thick disks characterized by $\nu = 2\alpha P/3\rho\Omega$ where the radiation field is a blackbody, the solution is

$$T = 2.28 \times 10^7 \alpha^{-1/4} M^{1/8} r^{-3/8} \text{ K} , \tag{17a}$$

$$\Sigma = 7.56 \times 10^2 \alpha^{-1}\dot{M}^{-1}M^{-1/2}r^{3/2}(1 - r^{-1/2})^{-1} \text{ g cm}^{-2} , \tag{17b}$$

and

$$H = 1.35 \times 10^4 \dot{M}(1 - r^{-1/2}) \text{ cm} \tag{17c}$$

for $P = P_{\rm rad} = aT^4/3$ and $\kappa_e \gg \kappa_{\rm ff}$ (denoted as regime I). In the case where the gas pressure dominates and $\nu = 2\alpha P_{\rm gas}/3\rho\Omega$ (regime II), the solution for $\kappa_e \gg \kappa_{\rm ff}$ is

$$T = 3.44 \times 10^7 \alpha^{-1/5}\dot{M}^{2/5}M^{3/10}r^{-9/10}(1 - r^{-1/2})^{2/5} \text{ K} , \tag{18a}$$

$$\Sigma = 3.95 \times 10^3 \alpha^{-4/5}\dot{M}^{3/5}M^{1/5}r^{-3/5} \times (1 - r^{-1/2})^{3/5} \text{ g cm}^{-2} \tag{18b}$$

and

$$H = 5.92 \times 10^3 \alpha^{-1/10}\dot{M}^{1/5}M^{-7/20}r^{21/20}(1 - r^{-1/2})^{1/5} \text{ cm} . \tag{18c}$$

Since the goal of our study is to examine the global response of the disk for different viscosity prescriptions, we also adopt a modified viscosity prescription in which the sound speed is determined by the gas pressure, but the scale height is given in terms of the total pressure (regime III). The solution in the limit that radiation pressure dominates is given by

$$T = 2.86 \times 10^7 \alpha^{-2/9}\dot{M}^{2/9}M^{2/9}r^{-2/3}(1 - r^{-1/2})^{2/9} \text{ K} , \tag{19a}$$

$$\Sigma = 1.89 \times 10^3 \alpha^{-8/9}\dot{M}^{-1/9}M^{-1/9}r^{1/3}(1 - r^{-1/2})^{-1/9} \text{ g cm}^{-2} , \tag{19b}$$

and

$$H = 1.35 \times 10^4 \dot{M}(1 - r^{-1/2}) \text{ cm} . \tag{19c}$$

The stability of accretion disks has been the subject of numerous investigations (Lightman and Eardley 1974; Shibazaki and Hoshi 1976; Shakura and Sunyaev 1976; Piran 1978; Sakimoto and Coriniti 1981). Solutions characterized by regimes I and III (see below) are unstable to density and thermal perturbations. The criterion for viscous instability as given by Lightman and Eardley (1974) and Pringle (1981) is

$$\frac{d}{d\Sigma}(v\Sigma) < 0 \tag{20}$$

or

$$\frac{dW}{d\Sigma} < 0\,, \tag{21}$$

where W is the integrated stress. As shown by Lightman and Eardley (1974), regime I is unstable to viscous processes since $W \propto \Sigma^n$, where $n < 0$. Instability to thermal processes is governed by

$$\left.\frac{d \log F^+}{d \log T}\right|_\Sigma > \left.\frac{d \log F^-}{d \log T}\right|_\Sigma, \tag{22}$$

where F^+ and F^- correspond to the local heating and cooling rates, respectively. The local stability analysis indicates that regime III is also viscously unstable. In addition, it is found that both regimes I and III are thermally unstable since the gas cannot radiate efficiently to achieve a thermal balance. To be complete, the disk solutions characterizing regime II are always stable.

IV. CALCULATIONS AND RESULTS

The partial differential thin disk equations describing mass and energy transport (eqs. [1] and [6]) have been solved using an explicit finite difference numerical method as outlined in Papaloizou, Faulkner, and Lin (1983). These equations were solved with the algebraic auxiliary relations given in § III. The inner region of the disk was divided into 35 radial zones with the inner (outer) boundary fixed at 3×10^6 (1.5×10^8) cm. No attempt is made to model the outer regions of the disk. Provided that the mass transfer rate is sufficiently high, the region of the disk immediately exterior to our outer boundary will be in a hot optically thick stable state (gas pressure dominated domain—regime II). The energy generation rate produced by viscous dissipation in this region (of a strong gravitational field) leads to conditions in the disk which are strongly stabilizing.

The parameters characterizing each of the model sequences is shown in Table 1. In the following we shall divide the discussion of the time-dependent disk evolution into two parts according to whether the global analysis indicates instability or stability of the disk.

a) Unstable Case

The viscosity prescription that is adopted corresponds to the standard case in which the total pressure determines both the local sound speed and the local scale height of the disk. As mentioned in § III the disk is unstable to surface density and thermal perturbations in the local approximation when the radiation pressure becomes dominant. If we define the quantity β as the ratio of the gas pressure to the total pressure ($P_{\rm gas}/P$), then the analysis of Shakura and Sunyaev (1976) shows that instability will develop when $1 - \beta$ exceeds 0.6. For a given accretion rate, $1 - \beta$ increases with decreasing distance of the disk from the central gravitating point mass and the instability is initiated in the inner region. The critical mass accretion rate, $\dot{M}_c$, as a function of the disk radius is given in Figure 1 for α equal to unity. For mass accretion rates in excess of the critical value (which is dependent on radius), the local analysis indicates that the disk will not be stable. From Figure 1 the inner disk is unstable for mass flow rates in excess of about 6×10^{16} g s^{-1}. For α different than unity, the critical mass accretion rates scale as $\alpha^{-1/8}$. For example, if α equals 0.1, the critical rates are increased by a factor of 33%. It should be noted that the condition for the onset of instability can also be described in terms of a critical surface density (see Fig. 1).

TABLE 1

MODEL SEQUENCES

Sequences	$\dot{M}$[a] (10^{18} g s^{-1})	C_s[b]	H[c]	Stability[d]
1.....	0.05	$(P/\rho)^{1/2}$	$(P/\rho)^{1/2}\frac{1}{\Omega}$	S
2.....	0.10	...	...	U
3.....	0.15	...	...	U
4.....	0.45	...	...	U
5.....	0.50	$(RT/\mu)^{1/2}$	$(P/\rho)^{1/2}\frac{1}{\Omega}$	S
6.....	1.00	...	...	S
7.....	1.00	$(RT/\mu)^{1/2}$	$(RT/\mu)^{1/2}\frac{1}{\Omega}$	S

[a] $\dot{M}$ = mass flow rate specified at the outer boundary of the disk.
[b] C_s = form adopted for the local sound speed.
[c] H = form adopted for the local pressure scale height.
[d] S = stable; U = unstable.

In order to study the time-dependent evolution of the disk in the radiation pressure dominated regime we first constructed an initial model (sequence 1) corresponding to a steady accretion disk. In particular, for a mass flow rate of 5×10^{16} g s^{-1}, we evolved a model disk for 411 s (comparable to the viscous diffusion time in our model) until a steady state was reached. The solution for the disk structure is in agreement (to within 10%) with that based upon the local approximation. To study the evolution of the disk in the regime predicted to be unstable by the local analysis the mass accretion rate, $\dot{M}_*$, at the outer boundary was increased by a factor of 2 to 10^{17} g s^{-1}. After about 750 s when all transient effects due to the initial model had decayed, a limiting state was reached. The accretion disk is not steady with the greatest variation in the mass transfer occurring in the inner regions. This variation leads to a sequence of bursts powered by the gravitational energy released in the infall process. At this point in the evolution, the amplitude and the recurrence time scale of the outburst have reached limiting values. The nonsteady flow is primarily confined to the inner 2.6×10^7 cm of the disk. In response to the increased mass flow rate at the outer boundary, the column densities and temperatures increase everywhere in the disk. When the column density and temperature increase to 1.14×10^3 g cm^{-2} and 1.07×10^7 K, respectively, at a radius of 3.4×10^6 cm, a thermal instability develops. The conversion of gravitational binding energy into thermal energy by the internal viscous stresses caused the local heating rate to exceed the local cooling rate, thereby, promoting an increase in the temperature. As a result, radiation pressure effects became important and because the viscosity prescription is a function of the total pressure, the viscosity became more temperature

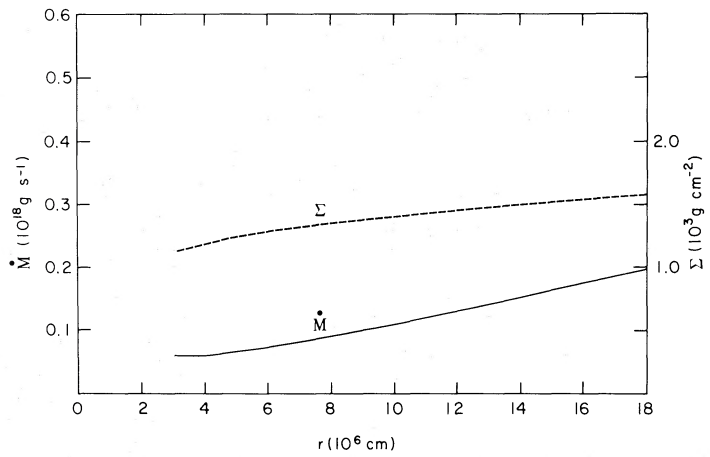

FIG. 1.—The critical mass accretion rate and surface density as a function of distance from the central object. Here the disk is characterized by the standard viscosity prescription with α equal to unity. The mass of the central object is assumed to be 1 $M_\odot$. For mass flow rates above this critical value, the local analysis predicts thermal and secular instability.

sensitive. This led to a further increase in the energy generation associated with viscous dissipation and to a thermal runaway. During this time the energy carried in the radial direction by advection and radiative heat transfer amounted up to 10% as compared with less than 0.5% in the quiescent state. The temperature at 3.4×10^6 cm initially rises to 1.57×10^7 K, thereby increasing the viscosity by about a factor of 7 to 8×10^{12} cm^2 s^{-1}, and then drops to 1.4×10^7 K as matter diffuses away more rapidly than can be replenished. The column density decreases to a temporary minimum value of 8.9×10^2 g cm^{-2}. The bulk of the matter flows to the neutron star surface at a velocity of about 2×10^7 cm s^{-1}, corresponding to rate of about 1.6×10^{18} g s^{-1}, and a small fraction flows outward at a velocity of 3×10^7 cm s^{-1} (mass flow rate of about 4×10^{18} g s^{-1}) to carry the angular momentum given up by the infalling matter. Global effects associated with advective terms in equation (1) and equation (6) lead to an increase of the mass flow rates in the regions immediately exterior to the unstable zones. These flows promote an increase in the column densities in these (initially) stable zones above the local critical value and, as a consequence, the region of instability spreads outward (see Fig. 2). As a result, most of the matter in these zones diffuses inward raising the temperatures to about 1.6×10^7 K and the column densities to 1.1×10^3 g cm^{-2}. It is during this phase that most of the energy is released. This energy is released primarily in the region interior to a radius of 5.4×10^6 cm. Two waves again emanate from the inner region, one propagating inward and the other outward. Since $\dot{M} > \dot{M}_c > \dot{M}_*$, matter in the inner disk is depleted. Within about 0.65 s after the onset of the burst, the temperature drops to 8.4×10^6 K as local cooling dominates local heating, thereby completing the outburst cycle. The runaway ceases at a point when the outward traveling wave cannot increase the column density above the local critical value required to initiate the thermal instability to maintain wave propagation. That is, the transition wave separating the radiation pressure dominant region (where $\beta < 0.4$) from the gas pressure dominant region (where $\beta > 0.4$) no longer propagates beyond the radius (about 2.6×10^7 cm in this case) where $\dot{M}_c > \dot{M}$. Thus the extent of the disk over which the instability can propagate is limited by the degree by which the disk deviates from the marginally unstable state (or, in other words, on the mass input rate, $\dot{M}_*$). The progress of the thermal runaway is determined by a competition between the rising temperatures associated with the high mass flow rates into the inner region from the outer part of the disk and the mass flow rates out of this region. Thus, the viscosity, in effect, limits the extent of the rise in temperature since the matter flows out of the unstable zones more rapidly during the outburst state. It should be noted that throughout the evolution of the burst the disk remains optically thick. In no case did any part of the calculated disk evolve into an optically thin state. Because the inner disk region is depleted, it is, again, replenished on its local viscous time scale. As a consequence the temperatures and column densities increase. After about 7 s, the development of the cycle begins anew as described above.

The temporal variation of the bolometric luminosity from

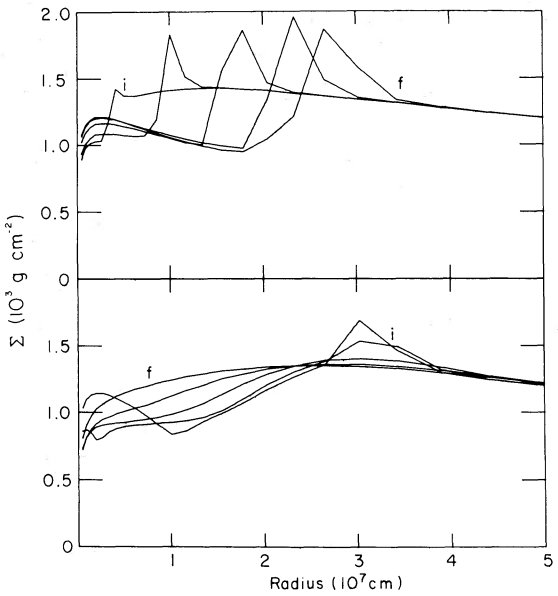

FIG. 2.—The distribution of the surface density for different times in the evolution of the disk during outburst. The upper panel illustrates the temporal variation of the surface density distribution as the wave propagates outward starting from an initial state, *i*, to a final state, *f*. In the lower panel the surface density distribution is plotted during the replenishment phase. Here *i* corresponds to the state immediately following the final state of the upper panel, and *f* corresponds to the final state.

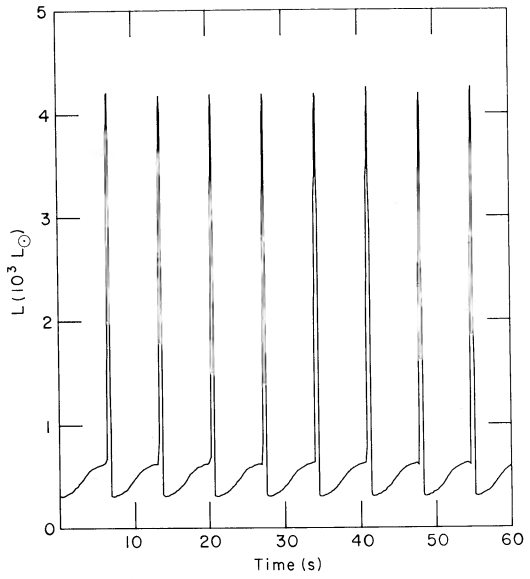

FIG. 3

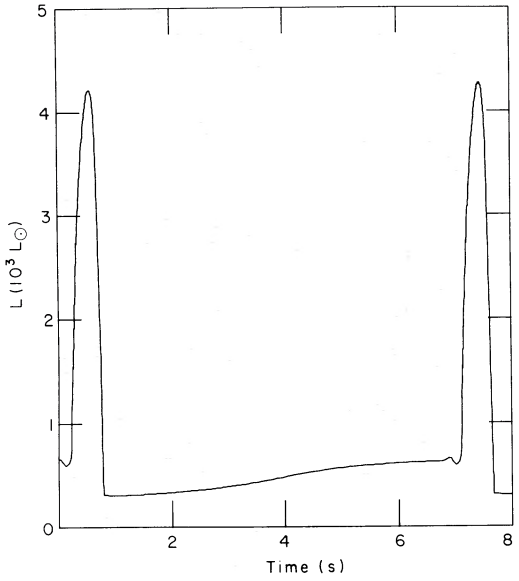

FIG. 4

FIG. 3.—Variation of the bolometric luminosity from the disk as a function of time (where the time has been reset to 0) for sequence 2 after a limiting cycle has been reached. The mass flow rate at the outer boundary of the disk corresponds to 10^{17} g s^{-1}.

FIG. 4.—Temporal variation of the bolometric luminosity from the disk for two successive bursts for sequence 2.

the disk is shown for a sequence of bursts in Figure 3, and a high-resolution plot of two bursts is shown in Figure 4. The rise time scale of the burst is 0.35 s, and the duration is 0.58 s. This variation reflects the slow rise and more rapid decline of the temperature (and hence the viscosity) in the inner region. If we define the emitting region to correspond to the area where the flux exceeds e^{-1} of the maximum value, then the effective temperature characterizing the peak of the burst is about 8.25×10^6 K. This emitting region extends to about 5.4×10^6 cm and does not vary significantly during the outburst. By integrating the luminosity over the burst duration we find that the total energy released in the burst is 7.26×10^{36} ergs. In addition, the ratio of the maximum luminosity to its premaximum value is 6.64. The recurrence time of the bursts is found to be 7.07 s with a ratio of the duration for the active to the inactive state of 0.09. The parameters characterizing the bursts are summarized for convenience in Table 2. From Figure 4, it is also seen that the quiescent level before the maximum is higher than the quiescent level immediately following the burst. This difference is a signature of this type of instability, and it is due to the fact that during the premaximum phase the inner region of the disk is building up, whereas after the burst, matter in the inner region has been depleted under the action of the elevated viscosity. It should be noted, however, that this signature may be masked by the X-ray radiation from the boundary layer or from the stellar surface.

In order to examine the sensitivity of the evolution to changes in the mass accretion rate at the outer boundary of the disk, we evolved the disk starting from the end of sequence 1 with a mass flow rate of 1.5×10^{17} g s^{-1} (sequence 3). After a limit cycle had been attained ($t \approx 350$ s), the evolution of the outburst is found to be similar in kind to that described for sequence 2 and to differ only in degree. The extent of the region which participated in the outburst increased from 2.6×10^7 cm in sequence 2 to 3×10^7 cm in sequence 3. The upward transition wave (initiated in the rising portion of the outburst) is found to propagate further outward since a greater fraction of the disk is near the critical state. Consequently, a greater part of the disk and, therefore, a greater amount of mass participated in the outburst. This demonstrates that the recurrence time scale of the outburst does not scale inversely with the accretion rate as would be expected if the mass involved in the outburst were constant. In particular the recurrence time scale decreases by a factor of 1.35, whereas the accretion rate was

TABLE 2

BURST CHARACTERISTICS

Sequence	τ_r(s)[a]	τ_d(s)[b]	τ_R(s)[c]	Q[d]	E(ergs)	L_m(ergs s^{-1})[e]	L_1(ergs s^{-1})[f]	L_2(ergs s^{-1})[g]
2.....	0.35	0.58	7.07	0.09	7.26(36)	1.66(37)	2.50(36)	1.25(36)
3.....	0.43	0.70	5.24	0.15	1.00(37)	1.95(37)	2.64(36)	1.32(36)
4[h].....	1.46	2.36	9.56	0.33	1.01(38)	6.64(37)	4.02(36)	1.88(36)

[a] τ_r = rise time of the burst.
[b] τ_d = duration of the burst.
[c] τ_R = recurrence time of the burst.
[d] Q = ratio of burst duration to the duration of the quiescent phase.
[e] L_m = peak burst luminosity.
[f] L_1 = luminosity level immediately prior to the onset of the burst.
[g] L_2 = luminosity level immediately following the termination of the burst.
[h] The burst characteristics are only indicative since a true limiting cycle has not been achieved—see text.

increased by a factor of 1.5. Because the affected region of the disk is greater in extent, the rise time and the duration of the burst are increased. This, combined with the increase in the peak luminosity (see Fig. 5), led to a greater energy release (10^{37} ergs). The main energy release is confined to a region about the same size as in sequence 2; hence, the effective temperature characterizing the peak of the outburst is about 8.6×10^6 K. It should be noted that the peak outburst luminosity appears to be correlated with the burst duration in the sense that the peak luminosity increases with increasing duration.

Since the variation in the mass flow rates for model sequences 2 and 3 differed by only 50% we increased the mass flow rate to 4.5×10^{17} g s^{-1} in sequence 4 (a factor of 9 times larger than the rate characterizing the steady state model). The disk was evolved for about 432 s at which time the disk had nearly reached a limiting state. In this sequence, it is found that the outward transition wave propagated to the outer boundary of our model disk. A true limiting state could be attained if we had extended the outer boundary of the disk to larger radii; however, the limitations imposed by the explicit method and the available computational resources made this an unrealistic goal. The results presented here, although preliminary, are probably indicative of the trends. The temporal variation of the luminosity of the disk is shown for two bursts in Figure 6. The correlation between the peak luminosity and the burst duration, found in sequence 3 is also evident for sequence 4. In particular, the peak luminosity and the burst duration increase to 6.65×10^{37} ergs s^{-1} and 2.36 s, respectively. On the other hand, the recurrence time scale is found to increase with increasing mass accretion rate. The recurrence time scale has increased to 9.56 s leading to the result that the duration of the active state is about one-third as long as the duration of the inactive (i.e., quiescent) state. The longer recurrence time scale is attributable to the fact that more of the disk is involved in the outburst and, therefore, a greater time is needed to replenish the inner regions. This demonstrates the intrinsic nonlinearity of the problem that is manifested in a global analysis and shows the inadequacy of local analysis in predicting such

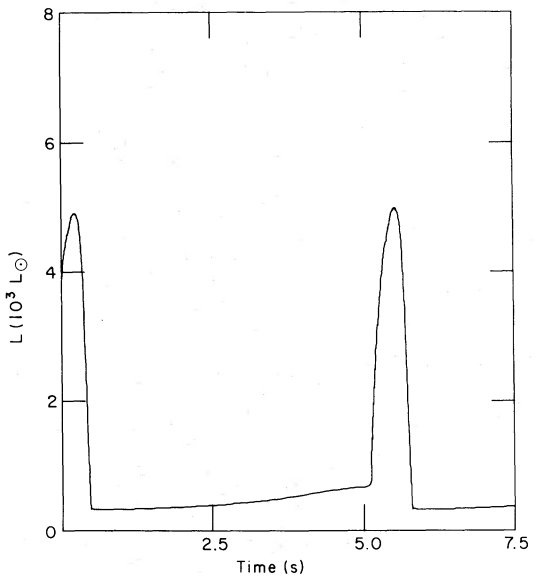

FIG. 5.—Variation of the bolometric luminosity as a function of time for sequence 3 ($\dot{M}_* = 1.5 \times 10^{17}$ g s^{-1}).

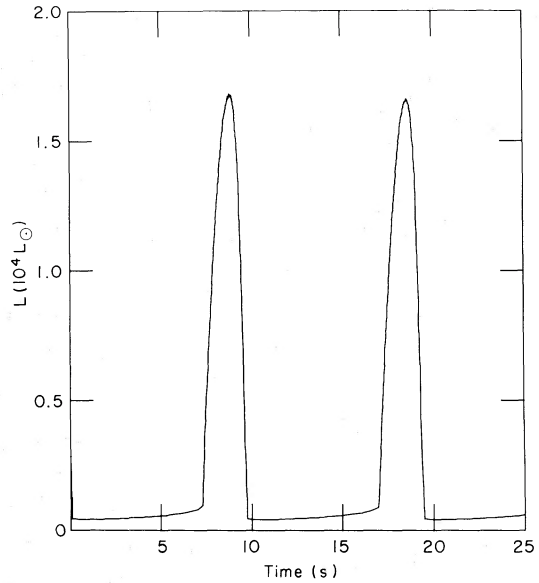

FIG. 6.—Temporal variation of the disk luminosity for sequence 4 ($\dot{M}_* = 4.5 \times 10^{17}$ g s^{-1}).

properties. For this sequence, the energy released and the peak effective temperature achieved in the outburst are 1.01×10^{38} ergs and 1.5×10^7 K, respectively.

To summarize, the local analysis approximately predicts the conditions necessary to initiate the thermal instability. The global analysis demonstrates that the instability does not coherently propagate throughout the entire disk, but only in the inner and intermediate regions. The region of the disk affected by the outburst increases in extent with increasing mass input rate in the disk. Throughout the evolution of the burst the calculated regions of the disk remain optically thick for all sequences. The peak burst luminosities and total energies are correlated with the burst duration but not with the recurrence time scale. The latter characteristic exhibits the intrinsic nonlinearity of the system. It should be mentioned that the properties listed in Table 2 are characteristic of a disk which has reached a limiting state, and deviations from these properties are possible, especially if the mass input rate at the outer boundary of our model disk varies on a time scale of the order of the viscous diffusion time characteristic of the quiescent state. In such circumstances, the outbursts will be characterized by irregular behavior.

b) Stable Case

For model sequences 5 and 6, we adopt a viscosity prescription such that the sound speed is given in terms of the gas pressure whereas the local scale height is given in terms of the total pressure (regime III). A local stability analysis of a disk described by such a viscosity prescription indicates that instability will develop for 1-β greater than 12/13 or for mass accretion rates in excess of about 5×10^{17} g s^{-1}. For sequences 5 and 6 which correspond to mass flow rates of 5×10^{17} g s^{-1} and 10^{18} g s^{-1}, respectively, it is found, in contrast to the case in regime I, that the disk evolves to a stable steady state. The stabilizing affect, is directly traceable to the importance of the non local energy transport processes. The advective and the radial heat transfer contribution were comparable to each other and, together, amounted to about 3% and 7% of the total energy transport for sequences 5 and 6 respectively. This

is to be compared to the less than 1% contribution in the evolution of the disk for sequence 1. The imbalance between the local heating and cooling was sufficient to stabilize the accretion disk. Typical values for β in the inner region were less than about 0.05 in the inner region and would have indicated instability in the local approximation. It is found that the global solution does not differ appreciably from that given by equation (18). In particular, the column density and the temperature are slightly greater by less than 10% and 5%, respectively. Our result, thus, reemphasizes the importance of the global analysis in the study of the structure and evolution of accretion disks.

For model sequence 7 we chose a viscosity prescription in which both the sound speed and the scale height of the disk are given in terms of the gas pressure alone. After evolving the disk for a viscous diffusion time scale, the disk evolves into a steady state as expected from the local analysis.

The two different viscosity prescriptions therefore lead to stable disks which are always optically thick everywhere. Our results indicate that the disk is stable if the local analysis indicates as such, but if instability is indicated by the local analysis, a global analysis is required to determine the outcome.

The difference between the evolution of the disk in sequences 2, 3, and 4 and sequences 5 and 6 is attributable to the fact that the viscosity is more temperature sensitive in the sequences for which the viscosity is given in terms of the total pressure. In particular, the energy generated by the viscous stresses is produced at a rate which is proportional to T^7 during the outburst state in sequences 2–4, whereas it is only proportional to $T^{4.3}$ for sequences 5 and 6. The maximum temperature dependences (obtained in the limit that β is zero) are T^8 and $T^{4.5}$ for the standard and modified viscosity prescription, respectively. This is to be compared with the temperature dependences of the rate of cooling which varies as T^4 for both cases. The different temperature dependencies in the heating and cooling rates for the modified prescription could be offset by the nonlocal energy flows, whereas the much greater differences for the standard case could not be offset.

V. CONCLUSIONS

This study has concentrated on the global response of a viscous accretion disk surrounding a neutron star subject to variations in the mass transfer rate either from a Roche lobe–filling star or from the outer disk on a time scale longer than the viscous diffusion time of the inner disk. It has been found that radial energy transport by advective processes and radiative diffusion can have important stabilizing affects on the disk structure and evolution. As a result, the instabilities inferred from a local analysis are not necessarily confirmed by a global analysis.

To study the nonlinearities of the accretion disk problem, we have examined several different viscosity prescriptions. In the case in which a modified description is used, we find from the local analysis that instability is predicted for accretion rates near the Eddington critical rate. Global analysis does not confirm this result as the nonlocal radial heat flow is sufficiently great to stabilize the inner region. On the other hand, the global analysis confirms the local analysis for the standard viscosity prescription. The instability manifests itself in the form of soft X-ray bursts ($kT < 2$ keV). In the latter study, the disk remains in an optically thick state. In addition, the disk is always geometrically thin with the scale height of the disk remaining less than about 0.1 times the radial distance from the center of the neutron star.

Our preliminary results indicate that a wide range of time scales for the bursts are possible and, in fact, display many of the gross features of the rapid X-ray burster (e.g., recurrent time scale, outburst magnitude, and characteristic spectral temperature). In particular, the recurrence time scale can be simply modulated by variation of the rate of the mass transfer into the inner region (e.g., due to a thermal instability in the partially ionized region in the outer parts of the disk). However, we have not attempted to compare our results with observations of celestial X-ray sources in detail. Caution is advised since the instabilities that we have studied are a result of the form of the viscous dissipation that we have adopted. Even if the short time scale transient behavior is due to such disk instabilities, the properties of the calculated bursts (for example, their shapes and time scales) can be easily changed by adopting a different viscosity prescription. Although the results are suggestive, a comparison with observations is not warranted at this time because of the major uncertainties underlying the physics of accretion disks. Further work on the nature of the viscosity in accretion disks will be needed before quantitative comparisons can be made.

This work was supported in part by NSF grants AST81-09826 A01, AST83-11406, and NASA grant NAGW-508. The authors gratefully acknowledge discussions with Dr. S. Woosley.

REFERENCES

Faulkner, J., Lin, D. N. C., and Papaloizou, J. 1983, *M.N.R.A.S.*, **205**, 359.
Illarionov, A. F., and Sunyaev, R. A. 1974, *Soviet Astr.–AJ*, **18**, 413.
Lamb, F. K., Fabian, A. C., Pringle, J. E., and Lamb, D. Q. 1977, *Ap. J.*, **217**, 197.
Lewin, W. H. G., *et al.* 1976, *Ap. J. (Letters)*, **207**, L95.
Lewin, W. H. G., and Joss, P. C. 1981, *Sp. Sci. Rev.*, **28**, 3.
Liang, E. P. T. 1977, *Ap. J. (Letters)*, **211**, L67.
Lightman, A. P. 1974, *Ap. J.*, **194**, 429.
Lightman, A. P., and Eardley, D. M. 1974, *Ap. J. (Letters)*, **187**, L1.
Lynden-Bell, D., and Pringle, J. E. 1974, *M.N.R.A.S.*, **168**, 603.
Meier, D. L. 1982, *Ap. J.*, **256**, 693.
Novikov, I., and Thorne, K. S. 1973, in *Black Holes, Les Houches 1973*, ed. C. DeWitt and B. DeWitt (New York: Gordon and Breach), p. 343.
Oda, M. 1982, in *Gamma Ray Transients and Related Astrophysical Phenomena*, ed. R. E. Lingenfelter, H. S. Hudson, and D. M. Worrall (New York: AIP), p. 319.
Papaloizou, J., Faulkner, J., and Lin, D. N. C. 1983, *M.N.R.A.S.*, **205**, 487.
Piran, T. 1978, *Ap. J.*, **221**, 652.
Prendergast, K. H., and Burbidge, G. R. 1968, *Ap. J. (Letters)*, **151**, L83.
Pringle, J. E. 1981, *Ann. Rev. Astr. Ap.*, **19**, 137.
Pringle, J. E., and Rees, M. J. 1972, *Astr. Ap.*, **21**, 1.
Pringle, J. E., Rees, M. J., and Pacholczyk, A. G. 1973, *Astr. Ap.*, **29**, 179.
Sakimoto, P. J., and Coroniti, F. V. 1981, *Ap. J.*, **247**, 19.
Shakura, N. I., and Sunyaev, R. A. 1973, *Astr. Ap.*, 24, 337.
———. 1976, *M.N.R.A.S.*, **175**, 613.
Shibazaki, N. and Hoshi, R. 1976, *Prog. Theoret. Phys.*, **54**, 706.
Tucker, W. H. 1975, in *Radiation Processes in Astrophysics* (Cambridge: MIT Press), p. 202.

D. N. C. LIN: Board of Studies in Astronomy and Astrophysics, Lick Observatory, University of California, Santa Cruz, CA 95064

RONALD E. TAAM: Department of Physics and Astronomy, Northwestern University, Evanston, IL 60201